

# Effective low-energy spin model for narrow zigzag graphene nanoribbons

V.O. Cheranovskii<sup>1</sup>, V.V. Slavin<sup>2</sup>, and E.V. Ezerskaya<sup>1</sup>

<sup>1</sup>*V.N. Karazin Kharkiv National University, 4 Svoboda Sq., Kharkiv 61022, Ukraine*  
E-mail: cheranovskii@i.ua

<sup>2</sup>*B. Verkin Institute for Low Temperature Physics and Engineering of the National Academy of Sciences of Ukraine*  
47 Nauky Ave., Kharkiv 61103, Ukraine

Received March 11, 2020, published online May 26, 2020

The magnetic properties of narrow zigzag graphene nanoribbons with periodically embedded atoms of transition metals have been studied in the framework of Heisenberg spin Hamiltonian. We have proposed the simple effective model to give a semi-qualitative description of the peculiarities of magnetization profiles of the systems under consideration. This model can be used for an arbitrary value of spin of the embedded atoms of transition metals. Our analytical and numerical calculations confirm the correctness of the proposed model.

Keywords: graphene nanoribbons, Lieb theorem, Heisenberg spin model.

## Introduction

Magnetic carbon-based materials like zigzag-edged graphene nanoribbons are considered as promising materials for future applications in graphene-based spintronic devices [1–3]. It is found both theoretically and experimentally that atoms of transition metals (ATM) may fill carbon vacancies in graphene clusters to form stable ATM-embedded structures. In contrast to pristine graphene nanoribbons, the theoretical description of the magnetic structure of these materials is based usually on different variants of density functional theory approach and the corresponding many-electron consideration is of big interest. One of the simplest variants of this consideration is based on the effective Heisenberg spin Hamiltonian approach [4–6], which permit us to perform the many-electron study of embedded structures with ATM of arbitrary spin.

In our recent work, we applied above approach to the study of the magnetic properties of some narrow graphene nanoribbons with periodically embedded ATM [7]. According to the extended Lieb theorem [8], these nanoribbons may have macroscopic ground-state spin. In particular, we studied the field dependence of the magnetization of the Heisenberg spin model for a simplest representative of zigzag nanoribbon–polyacene macromolecule by means of the quantum Monte Carlo (QMC) method based on stochastic series expansion approach [9]. We expected to obtain a monotonic increase of the magnetization of pristine polyacene

with the increase of the external magnetic field. For ATM-embedded polyacene, we suppose to find the intermediate plateau in field dependence of magnetization because in the case of nonmagnetic ATM ( $s = 0$ ) the Hamiltonian (1) corresponds to so-called polyallyl spin chain having one intermediate magnetization plateau [10]. Unexpectedly, we found numerically at low temperatures one intermediate plateau for pristine polyacene macromolecule and two intermediate plateaus for embedded polyacene derivatives despite the absence of small interactions between site spins.

In several research papers [11,12] the magnetic properties of pristine graphene nanoribbons with zigzag edge termination were treated with the help of effective two-leg spin-1/2 ladder model with ferromagnetic interactions along the legs and antiferromagnetic interactions in rungs. In this work, we applied a similar idea in order to give a simple semi-qualitative description of the peculiarities of magnetization profiles of the Heisenberg spin models for narrow zigzag graphene nanoribbons with periodically embedded ATM of arbitrary spin.

## Effective low-energy spin Hamiltonian for polyacene derivatives

Carbon atoms of the pristine polyacene macromolecule are arranged in the stripe of hexagons. Quasihomopolar energy states of  $\pi$ -electron network of this macromolecule can be described adequately by effective Heisenberg spin-1/2 Hamiltonian on the corresponding hexagonal lattice stripe [4,5].

According to Lieb theorem [13], this Hamiltonian has a singlet ground state. Let us enumerate all the atoms consequently along the unit cells and consider the polyacene derivative for which all the fourth carbon atoms of each unit cell are substituted by the ATM of spin  $s$  (Fig. 1).

The spin Hamiltonian of this polyacene derivative in presence of the external magnetic field  $h$  has the following form:

$$\mathbf{H} = J \sum_{n=1}^L \left( \sum_{k=1}^3 \mathbf{S}_{n,k} \mathbf{S}_{n,k+1} + \mathbf{S}_{n,1} \mathbf{S}_{n+1,1} + \mathbf{S}_{n,4} \mathbf{S}_{n+1,4} \right) - h \sum_{n=1}^L \sum_{k=1}^4 \mathbf{S}_{n,k}^z. \quad (1)$$

Here, for simplicity of further consideration, we put equal coupling constants for all the interactions between neighbor spins of the lattice; the spin operator  $\mathbf{S}_{n,4}$  corresponds to the embedded ATM spin of the  $n$ th unit cell.

For finite fragment of above lattice structure formed by  $L$  unit cells, according to the extended Lieb theorem, the Heisenberg spin model has the ground-state spin  $S_0 = L(s - 1/2)$ , which takes macroscopic value in the limit  $L \rightarrow \infty$  at  $s \neq 1/2$ . According to the Klein theorem [8], for the ground-state  $\Psi_0$  the two-particle correlators  $\langle i-j \rangle = \langle \Psi_0 | S_i S_j | \Psi_0 \rangle$  for embedded spins with  $s \neq 0$  have positive values. A similar consideration is valid for opposite carbon spins (site spins with numbers  $(n, 1)$ ). The spin correlators for marginal spins of the same unit cell (embedded spin  $s$  and opposite carbon spin) should have a negative sign. In other words, we may say about effective ‘‘ferromagnetic’’ ordering of the marginal spins along the polyacene zigzag edges and antiferromagnetic interactions between the marginal spins of different zigzag edges. There are also  $L$  pairs of spins which belongs to two neighbor hexagons simultaneously (vertical edges of the lattice graph). According to [8], the corresponding spin correlators should have a negative sign.

Similar to [11,12] the set of marginal spins of the nanoribbon can be described by the effective two-leg spin ladder with ‘‘ferromagnetic’’ interactions in legs and ‘‘antiferromagnetic’’ interactions in rungs. Due to the topology of the hexagon stripe, the diagonal interactions of the marginal spins should be taken into account. As a result, for the simulation of the magnetic properties of the embedded nanoribbons, instead of full Heisenberg spin Hamiltonian of the polyacene derivative stripe of size  $L$ , we may treat the simple low-energy model — two-leg mixed spin ladder formed by  $L$  unit cells with diagonal interactions and  $L$  isolated pair of spin 1/2 with effective antiferromagnetic interaction (Fig. 2).

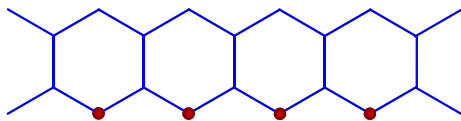


Fig. 1. Polyacene with embedded ATM of spin  $s$  (balls).

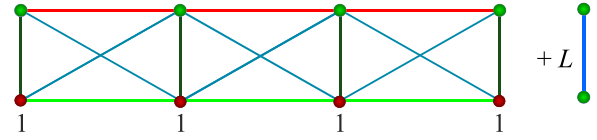


Fig. 2. (Color online) Effective low-energy spin model for description of the magnetization profile of polyacene macromolecule with embedded ATM (red balls, 1).

The corresponding Heisenberg spin Hamiltonian has the form

$$\mathbf{H}_{\text{eff}}(L, h) = L \left( J_0 \mathbf{S}_1 \mathbf{S}_2 - h \mathbf{S}_1^z - h \mathbf{S}_2^z \right) + \mathbf{H}_{\text{ladder}}(L, h), \quad (2)$$

where

$$\begin{aligned} \mathbf{H}_{\text{ladder}}(L) = & \sum_{n=1}^{L-1} \left[ J_1 \mathbf{S}_{1,n} \mathbf{S}_{1,n+1} + J_2 \mathbf{S}_{2,n} \mathbf{S}_{2,n+1} + J_3 \mathbf{S}_{1,n} \mathbf{S}_{2,n} + \right. \\ & \left. + J_4 \left( \mathbf{S}_{1,n} \mathbf{S}_{2,n+1} + \mathbf{S}_{1,n+1} \mathbf{S}_{2,n} \right) \right] + \\ & + J_0 \mathbf{S}_{1,L} \mathbf{S}_{2,L} - h \sum_{n=1}^L \left( \mathbf{S}_{1,n}^z + \mathbf{S}_{2,n}^z \right), \quad J_1, J_2 < 0, \quad J_3, J_4 > 0. \end{aligned}$$

Here the spin operator  $\mathbf{S}_{1,n}$  corresponds to the spin 1/2 located on the  $n$ th site of the upper leg of the ladder and  $\mathbf{S}_{2,n}$  corresponds to the spin  $s$  located on the  $n$ th site of the bottom leg. For pristine polyacene  $J_1 = J_2$ .

The energy spectrum of the effective spin ladder can be estimated analytically in the linear spin-wave approximation (see Appendix) or numerically by means of density matrix renormalization group (DMRG) approach and by the quantum Monte Carlo method. Due to ferromagnetic coupling in legs, our spin ladder model has nonfrustrated character and obeys the Lieb theorem. According to the simple generalization of Lieb theorem [13], there is a following ordering of lowest energy states with specified values of total spin  $S$ :

$$E_{\min}(S+1) > E_{\min}(S), \quad S \geq S_0 = L(s - 1/2). \quad (3)$$

Therefore the external magnetic field will increase smoothly total magnetization up to the value, which corresponds to  $z$ -projection of a total spin of the embedded polyacene  $M_1 = L(2s+1)/4$ , if the coupling parameter  $J_0$  satisfies the condition

$$J_0 > E_{\min}(S_0 + n) - E_{\min}(S_0 + n - 1), \quad n = 1, 2, \dots, L. \quad (4)$$

Further increase of the external field leads to the triplet excitations inside the isolated pairs of spins and at  $h > J_0$  we obtain the state with maximal magnetization. As a result, the field dependence of the total magnetization of the spin system (2) should have an intermediate plateau at  $z$ -projection of the total spin per unit cell  $m = s + 1/2$ . For the polyacene embedded by ATM with  $s > 1/2$ , the effective ladder Hamiltonian has the macroscopic ground-state spin and we may expect the existence of additional inter-

mediate plateau at  $m = s - 1/2$  due to the possible gapped character of the lowest excitations with total spin  $S > S_0$ .

In order to check the adequacy of the proposed model, we studied numerically by DMRG method the spin correlator  $R = \langle n, 2-n, 3 \rangle$  for pair of spins corresponding to vertical edges of the polyacene graph. According to our model, the lowest energy state of the Hamiltonian (1) from the subspace the value with  $m = s + 1/2$  should correspond to the beginning of the magnetization plateau. Therefore, the above spin correlator for this state should have a preferably antiferromagnetic character. Our DMRG simulations give  $R = -0.483, -0.481, \text{ and } -0.392$  for polyacene structures with  $s = 1/2, 1, \text{ and } 3/2$ , respectively. These results may be treated approximately as the presence of localized singlet pair of spins located on the vertical edges of the lattice graph.

To estimate the effective coupling constant of the Hamiltonian (2) let us suppose, that in the lowest energy state of (2) with  $m = s + 1/2$  there is perfect singlet coupling for pairs of spins located on vertical edges of the lattice graph. The energy of this state has the form

$$E_1 = L \left[ (J_1 + J_2 + J_3 + 2J_4) / 4 - 3J_0 / 4 \right]. \quad (5)$$

The state with the maximal value of total spin has the energy

$$E_f = L \left[ (J_1 + J_2 + J_3 + 2J_4) / 4 + J_0 / 4 \right]. \quad (6)$$

Similar to [4,6], we may estimate the coupling constant  $J_0$  using the corresponding exact energies of the Hamiltonian (1) for finite lattice fragment. There are different ways to do this. We used for all polyacene derivatives the fragment formed by two hexagons which corresponds to the system formed by one four-spin fragment of the effective ladder model and three isolated pairs of interacting spins  $1/2$  (Fig. 3). As a result, we have

$$J_0 = (\bar{E}_f - \bar{E}_1) / 3, \quad (7)$$

where  $\bar{E}_f$  and  $\bar{E}_1$  are the exact energies of two-hexagon fragment described by the Hamiltonian (1) for ferromagnetic state and the lowest energy state with  $m = s + 1/2$ , respectively. From the topology of this fragment, we may also suppose the following relation:  $J_3 = 2J_4$ .

Similarly, we estimated the effective coupling constant  $J_3$  using two lowest energy states of the four-site unit cell

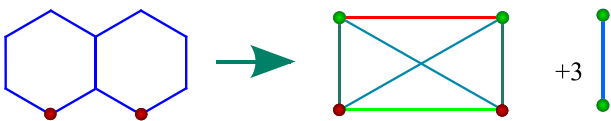


Fig. 3. (Color online) 10-spin fragment of polyacene derivative and the corresponding effective spin model.

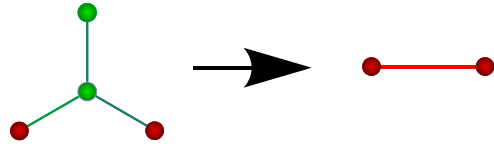


Fig. 4. (Color online) Four-sites fragment of the polyacene with two embedded heteroatoms and the corresponding effective two-spin system.

$\varepsilon_0$  and  $\varepsilon_1$  of the initial spin system described by the Hamiltonian (1):

$$J_1 = (\varepsilon_1 - \varepsilon_0) / (s + 1/2). \quad (8)$$

For the estimation of ferromagnetic interactions along the ladder legs from the lowest energy levels  $\varepsilon_{\min}(2s)$  and  $\varepsilon_{\min}(2s-1)$  of the following four-site polyacene fragment (Fig. 4).

The Hamiltonian of this fragment has a simple energy spectrum, which can be found analytically for arbitrary  $s$ . In particular,  $\varepsilon_{\min}(2s) = -(s + 3/4)J$  and  $\varepsilon_{\min}(2s-1) = -(s + 1/4)J$ . As a result, we obtain a negative coupling constant describing the interaction of two ATM spins  $J_1 = -J / (4s)$ .

We applied the above scheme to polyacene with ATM of spin  $s = 1/2, 1, \text{ and } 3/2$ . The effective coupling parameters for the Hamiltonian (2) are given in the unit of  $J$  in Table 1.

Table 1. Effective coupling parameters for the Hamiltonian (2)

$s$	$J_0$	$J_1$	$J_2$	$J_3$
1/2	1.99	-0.5	-0.5	0.659
1	2.45	-0.5	-0.25	0.513
3/2	3.03	-0.5	-0.167	0.402

### Numerical simulation of magnetization profiles

Nonfrustrated character of the spin ladder Hamiltonian permits us to use QMC method for the numerical simulation of their low-temperature thermodynamics. For the check, we also used the density matrix renormalization group method at zero temperature [14]. All the QMC calculations were performed at temperature  $T = 0.02$  (in unit of  $J$ ) and the systems size  $N = 1200$  spins. The corresponding DMRG calculations were done at  $N = 400$  spins and 50 optimized states. Besides, our DMRG calculations indicate that in the ground-state spin-spin correlators of neighbor spins have positive (ferromagnetic) sign in legs and have a negative (antiferromagnetic) sign in rungs. This result also confirms the correctness of the proposed model (see [11,12]).

On Figs. 5–7 we presented the magnetization profiles of polyacene macromolecules with ATM of spin  $s = 1/2, 1, 3/2$ , respectively (the case  $s = 1/2$  corresponds to pristine polyacene). For all the figures curves 1 correspond to QMC calculations for the Hamiltonian (1), curves 2 with

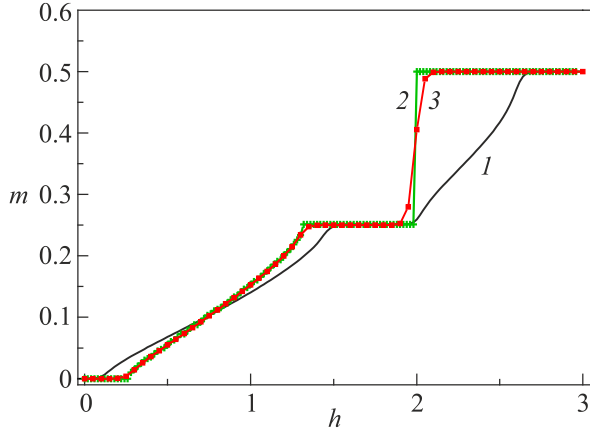


Fig. 5. (Color online) Magnetization profile with one intermediate magnetization plateau for pristine polyacene macromolecule.

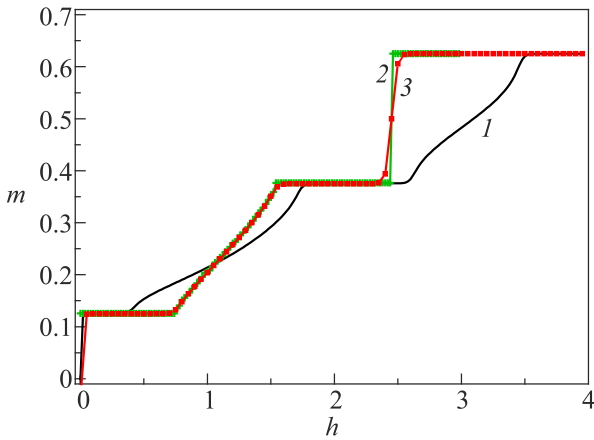


Fig. 6. (Color online) Magnetization profile with two intermediate magnetization plateaus for polyacene macromolecules with ATM spin  $s = 1$ .

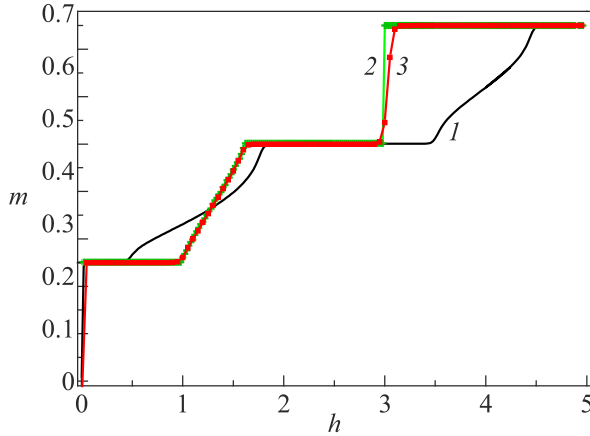


Fig. 7. (Color online) Magnetization profile with two intermediate magnetization plateaus for polyacene macromolecules with ATM spin  $s = 3/2$ .

crosses and curves 3 with filled boxes are the magnetization profiles for the model (2) calculated by DMRG and QMC methods, respectively.

## Conclusions

We have proposed an effective simple model to describe magnetic properties of narrow zigzag graphene nanoribbons with periodically embedded ATM. The model consists of two-leg ladder with diagonal interactions and the set of  $S = 1/2$  isolated dimers. One leg of the ladder contains  $S = 1/2$  spins and other leg contains ATM spins. The parameters of effective coupling can be obtained analytically from the analysis of a small fragment of the initial system. Our analytical and numerical calculations have been shown that the effective model describes adequately the main peculiarities of the magnetization profile of narrow zigzag graphene nanoribbons with periodically embedded ATM. It should be noted, that the proposed approach can be extended to the polyacene derivatives with periodically embedded ATM of more complicated structure, e.g., nanoribbons formed by two chains of hexagons.

## Appendix

We consider spin ladder with two different antiferromagnetic (AF) interactions in legs ferromagnetic (FM) interaction in rungs with Hamiltonian

$$\hat{\mathbf{H}} = \sum_{n=1}^N \left[ -J_1 \mathbf{S}_{1,n} \mathbf{S}_{1,n+1} - J_2 \mathbf{S}_{2,n} \mathbf{S}_{2,n+1} + J_3 \mathbf{S}_{1,n} \mathbf{S}_{2,n} + J_4 (\mathbf{S}_{1,n} \mathbf{S}_{2,n+1} + \mathbf{S}_{1,n+1} \mathbf{S}_{2,n}) \right]. \quad (\text{A.1})$$

Here  $J_i > 0$ ,  $i = 1, \dots, 4$ , and  $N$  is the number of spins in each chain (leg). Leg spins are  $s_1$  and  $s_2$ . We assume the periodic boundaries, which means  $\mathbf{S}_{jN+1} = \mathbf{S}_{j1}$ ,  $j = 1, 2$ .

Let us start from AF ground state, and consider (A.1) in linear spin-wave approximation. According well known Holstein–Primakoff transformation,

$$\begin{aligned} S_{1,n}^+ &\approx \sqrt{2s_1} a_{1,n}, & S_{1,n}^z &= s_1 - a_{1,n}^\dagger a_{1,n}; \\ S_{2,n}^+ &\approx \sqrt{2s_2} a_{2,n}^\dagger, & S_{1,n}^z &= a_{2,n}^\dagger a_{2,n} - s_2. \end{aligned} \quad (\text{A.2})$$

Linearized Hamiltonian (A.1) has the form

$$\begin{aligned} \hat{\mathbf{H}}_0 = E_0 + \sum_{n=1}^N &\left\{ (J_3 s_2 + 2J_1 s_1) a_{1,n}^\dagger a_{1,n} + (J_3 s_1 + 2J_2 s_2) a_{2,n}^\dagger a_{2,n} + \right. \\ &\left. + \left[ -(J_1 s_1 a_{1,n}^\dagger a_{1,n+1} + J_2 s_2 a_{2,n}^\dagger a_{2,n+1}) + \right. \right. \\ &\left. \left. + \sqrt{s_1 s_2} \left( J_3 a_{1,n}^\dagger a_{2,n}^\dagger + J_4 (a_{1,n}^\dagger a_{2,n+1}^\dagger + a_{1,n+1}^\dagger a_{2,n}^\dagger) \right) + \text{h.c.} \right] \right\}, \end{aligned} \quad (\text{A.3})$$

where  $E_0 = -\left[ J_1 s_1^2 + J_2 s_2^2 + (J_3 + 2J_4) s_1 s_2 \right] N$  is the AF ground-state energy.

Translation symmetry in the horizontal direction permits us to introduce quasi-wave vector  $k = 2\pi l / N$ ,

$l = 0, 1, \dots, N-1$ , perform Fourier transformation of  $a_{1n}, a_{2n}$  in (A.3)

$$a_{1n} = \frac{1}{\sqrt{N}} \sum_k \exp(ikn) a_{1,k}, \quad a_{2n} = \frac{1}{\sqrt{N}} \sum_k \exp(-ikn) a_{2,k}, \quad (\text{A.4})$$

and rewrite (A.3) as

$$\begin{aligned} \hat{\mathbf{H}}_0 = E_0 + \sum_k \left\{ \left[ (J_3 + 2J_4)s_2 - 4J_1s_1 \sin^2\left(\frac{k}{2}\right) \right] a_{1,k}^\dagger a_{1,k} + \right. \\ \left. + \left[ (J_3 + 2J_4)s_2 - 4J_1s_1 \sin^2\left(\frac{k}{2}\right) \right] a_{2,k}^\dagger a_{2,k} + \right. \\ \left. + \sqrt{s_1s_2} (J_3 + 2J_4 \cos k) (a_{1,k}^\dagger a_{2,k}^\dagger + \text{h.c.}) \right\}. \quad (\text{A.5}) \end{aligned}$$

For diagonalization of (A.5) one can use the Heisenberg representation of the creation and annihilation operators to derive the equations of movement:

$$\dot{a}_{jk} = \frac{i}{\hbar} [\hat{\mathbf{H}}_0, a_{jk}], \quad j = 1, 2. \quad (\text{A.6})$$

Generalized  $u$ - $v$  Bogolubov transformation has the form

$$a_{jk} = \sum_{l=1}^2 \left( U_{lk}^{(j)} b_{lk} + V_{lk}^{(j)*} b_{lk}^\dagger \right), \quad j = 1, 2. \quad (\text{A.7})$$

Because a new set of operators  $b_{i,k}, b_{i,k}^\dagger$  should diagonalize the Hamiltonian (A.5), we have

$$\dot{b}_{lk} = -\frac{i}{\hbar} \varepsilon_k^{(l)} b_{lk}. \quad (\text{A.8})$$

For each  $\varepsilon_k^{(l)}$  we have similar sets of 8 linear uniform algebraic equations for 8 coefficients, which separate into four sets with 2 equations corresponding to two energy branches. One should take only non-negative energies (excitations above the ground state)

$$\begin{aligned} \varepsilon_k^{(1,2)} = \frac{1}{2} \left\{ \pm \left[ (J_3 + 2J_4)(s_2 - s_1) + 4(J_1s_1 - J_2s_2) \sin^2\left(\frac{k}{2}\right) \right] + \right. \\ \left. + \sqrt{\left[ (J_3 + 2J_4)(s_2 + s_1) + 4(J_1s_1 + J_2s_2) \sin^2\left(\frac{k}{2}\right) \right]^2 - 4(J_3 + 2J_4 \cos k)^2 s_1s_2} \right\}. \quad (\text{A.9}) \end{aligned}$$

It is easy to see that for  $k = 0$  in (A.9) zero energy  $\varepsilon = 0$  exists always. It means that in linear spin-wave approximation the energy spectrum is gapless. In the long-wave limit  $k \ll 1$  the approximation formulas for lowest energies are: at  $s_1 \neq s_2$

$$\varepsilon_k \approx \left( \frac{J_1s_1^2 + J_2s_2^2 + 2J_4s_1s_2}{|s_1 - s_2|} \right) k^2 \quad (\text{A.10})$$

and at  $s_1 = s_2 = s$

$$\varepsilon_k \approx s \sqrt{(J_1 + J_2 + 2J_4)(J_3 + 2J_4)} |k|. \quad (\text{A.11})$$

It should be noted, that the approximate formula (A.10) does not depend on AM interaction in rungs  $J_3$ .

1. G. Magda, X. Jin, I. Hagymási, P. Vancsó, Z. Osváth, P. Nemes-Incze, C. Hwang, L.P. Biró, and L. Tapasztó, *Nature* **514**, 608 (2014).
2. S. Yang, J. Li, and S.-S. Li, *Chin. Phys.* **27**, 117102 (2018).
3. G. Yu, X. Lü, L. Jiang, W. Gao, and Y. Zheng, *J. Phys. D* **46**, 375303 (2013).
4. L.N. Bulaevskii, *Z. Eksp. Teor. Fiz.* **51**, 230 (1966).
5. A.A. Ovchinnikov, *Theor. Chim. Acta* **47**, 297 (1978).
6. V.O. Cheranovskii, E.V. Ezerskaya, D.J. Klein, and A.A. Kravchenko, *J. Magn. Magn. Mater.* **323**, 1636 (2011).
7. V.O. Cheranovskii, V.V. Slavin, E.V. Ezerskaya, A.L. Tchougreeff, and R. Dronskowski, *Crystals* **9**, 251 (2019).
8. D.J. Klein, *J. Chem. Phys.* **77**, 3098 (1982).
9. A.W. Sandvik, *Phys. Rev. B* **59**, R 14157 (1999).
10. V.O. Cheranovskii and I. Özkan, *J. Magn. Magn. Mater.* **223**, 156 (2001).
11. M.J. Schmidt, M. Golor, T.C. Lang, and S. Wessel, *Phys. Rev. B* **87**, 24531 (2013).
12. C. Koop and S. Wessel, *Phys. Rev. B* **96**, 165114 (2017).
13. E.H. Lieb and D.C. Mattis, *J. Math. Phys.* **3**, 749 (1962).
14. S.R. White, *Phys. Rev. Lett.* **69**, 2863 (1992).

**Ефективна низькоенергетична спінова модель  
для вузьких зигзагоподібних графенових  
нанострічок**

**В.О. Черановський, В.В. Славін, Е.В. Єзерська**

У рамках спінового гамільтоніану Гейзенберга досліджено магнітні властивості вузьких зигзагоподібних графенових нанострічок з періодично вбудованими атомами перехідних ме-

талів. Запропоновано ефективну просту модель, що дозволяє напівякісно описати особливості профілів намагніченості розглянутих систем. Ця модель може бути використана при доволіному значенні спіну вбудованих атомів перехідних металів. Аналітичні та числові розрахунки підтверджують адекватність запропонованої моделі.

Ключові слова: графенові нанострічки, теорема Ліба, спінова модель Гейзенберга.